

RESEARCH PAPER

## Optical Constants and Dispersion Parameters of $(\text{NiO})_{1-x}(\text{Co}_3\text{O}_4)_x$ Nano Composite Thin Films Prepared by Chemical Spray Pyrolysis

Huda R. Abdulridha Mohammed <sup>\*</sup>, Nahida B. Hasan, Mohammed Hadi Shinen

Department of Physics, College of Science, University of Babylon, Iraq

### ARTICLE INFO

#### Article History:

Received 02 September 2025

Accepted 23 October 2025

Published 01 January 2026

#### Keywords:

Cobalt oxide

Energy gap

Nanocomposite

Nickel oxide

### ABSTRACT

A 0.05 M  $\text{NiCl}_2 \cdot 6\text{H}_2\text{O}$  and 0.05 M  $\text{CoCl}_2 \cdot 6\text{H}_2\text{O}$  dissolved in distilled water to make it ready for next step of our preparation were used to produce  $(\text{NiO})_{1-x}(\text{Co}_3\text{O}_4)_x$  nano composite thin films on a glass substrate using a spray pyrolysis process. With increasing  $\text{Co}_3\text{O}_4$  concentration, the reflectivity, real and imaginary dielectric constants, and refractive index all increased. This may be due to the homogeneity and surface roughness of the films, a result that is beneficial for gas sensor applications. The energy difference decreased from (3.75 to 2.1) eV. With increasing  $\text{Co}_3\text{O}_4$  concentration in the  $(\text{NiO})_{1-x}(\text{Co}_3\text{O}_4)_x$  composite thin films, the dispersion coefficients decreased also. Energy dispersive X-ray spectroscopy (EDX), the analysis revealed the prominent presence of the components Ni, O, and Co. The field emission scanning electron microscopy (FESEM) confirmed our prepared surface it is agglomerate and nanosurface, It can be noted thin films have a common surface shape comprising many randomly placed chunks or aggregates of  $\text{Co}_3\text{O}_4$  on the top surface of the films.

### How to cite this article

Mohammed H., Hasan N., Shinen M. Optical Constants and Dispersion Parameters of  $(\text{NiO})_{1-x}(\text{Co}_3\text{O}_4)_x$  Nano Composite Thin Films Prepared by Chemical Spray Pyrolysis. J Nanostruct, 2026; 16(1):188-197. DOI: 10.22052/JNS.2026.01.017

### INTRODUCTION

A material's optical characteristics define its relationship to light. Reflectance, absorption, dispersion transmittance, and refractive index are among the material's optical characteristics [1].

With a large band gap (3.6-4.0) eV [2], ferromagnetic characteristics, a working temperature of 523 K, and a p-type semiconductor that has demonstrated remarkable chemical stability, nickel oxide is a green crystalline solid. It has been the subject of numerous scientific studies due to its unique electrical, magnetic, and optical characteristics.

It was an interesting research material

because of its excellent ion storing qualities and low cost. NiO nanostructures, for example, are p-type semiconductors with peculiar electric and magnetic characteristics that change depending on the particle size [3].

Cobalt oxide is one of the most researched oxide materials because of its uses in many different technological fields, including the absorber layer in solar cells [4], dye for ceramics and glass [5], electrode for electrochemical devices [6], gas sensors [7,8], super capacitors [9], smart glasses, and electrochemical devices [9,10]. The three distinctive crystalline phases of cobalt oxide are

<sup>\*</sup> Corresponding Author Email:

huda.mohammed@student.uobabylon.edu.iq



This work is licensed under the Creative Commons Attribution 4.0 International License.

To view a copy of this license, visit <http://creativecommons.org/licenses/by/4.0/>.

cobalt(II) oxide ( $\text{CoO}$ ), cobalt(III) oxide ( $\text{Co}_2\text{O}_3$ ), and cobalt(II,III) oxide ( $\text{Co}_3\text{O}_4$ ). Since cobalt can absorb oxygen (O) even at room temperature, high temperatures (about 1173 K) are required to make pure cobalt oxide.  $\text{Co}_2\text{O}_3$  completely transforms into  $\text{Co}_3\text{O}_4$  without changing its lattice structure when sufficient oxygen is collected at temperatures higher than 573 K [11–13]. Thin films of the composite  $(\text{NiO})_{1-x}(\text{Co}_3\text{O}_4)_x$  were prepared in this investigation using the spray pyrolysis process.

## MATERIALS AND METHODS

Spray pyrolysis was used to create the  $(\text{NiO})_{1-x}(\text{Co}_3\text{O}_4)_x$  composite thin films on a glass substrate. The spraying solution was prepared from 0.05 M of  $\text{NiCl}_2 \cdot 6\text{H}_2\text{O}$  and 0.05 M of  $\text{CoCl}_2 \cdot 6\text{H}_2\text{O}$  dissolved in 100 ml distilled water.  $(\text{NiO})_{1-x}(\text{Co}_3\text{O}_4)_x$  composite thin films prepared with various concentration (0, 25, 50, 75, 100)%, Fig. 1 shows solutions with different volume ratios (A-  $\text{NiO}$  pure, B-  $(\text{NiO})_{75}(\text{Co}_3\text{O}_4)_{25}$ , C-  $(\text{NiO})_{50}(\text{Co}_3\text{O}_4)_{50}$ , D-  $(\text{NiO})_{25}(\text{Co}_3\text{O}_4)_{75}$



Fig. 1. Images of solutions for  $(\text{NiO})_{1-x}(\text{Co}_3\text{O}_4)_x$  at various volumes of (x).

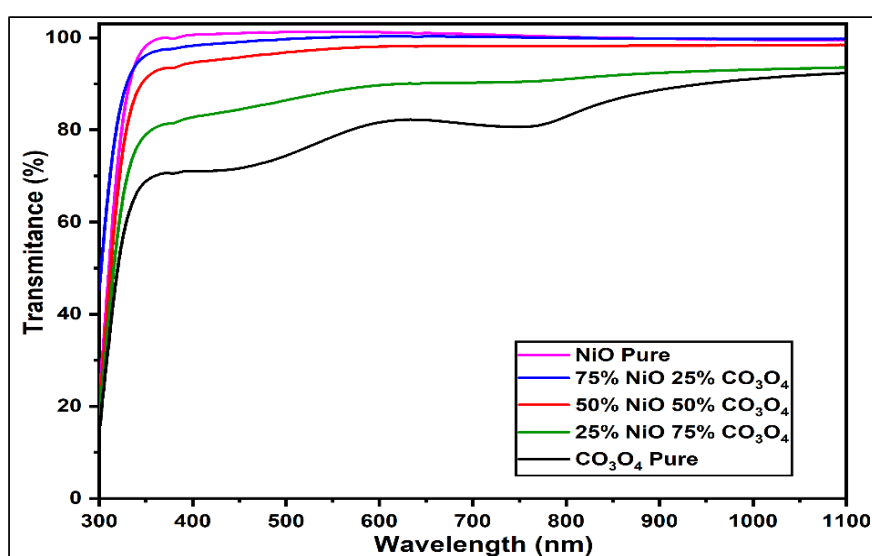


Fig. 2. Spectrum of transmittance for  $(\text{NiO})_{1-x}(\text{Co}_3\text{O}_4)_x$  composite thin films at varying percentages of (x).

and E-  $\text{Co}_3\text{O}_4$  pure) depending on the value  $x$  in  $(\text{NiO})_{1-x}(\text{Co}_3\text{O}_4)_x$ .

The deposition parameters, including the stopping time of two minutes, the deposition rate of two milliliters per minute, and the space between the nozzle and the substrate of thirty centimeters, were maintained at optimal values. A UV-visible spectrophotometer is used to calculate certain optical parameters and record absorption spectra in the (300–1100) nm range.

## RESULTS AND DISCUSSION

### Optical Constants

Fig. 2 displays the  $(\text{NiO})_{1-x}(\text{Co}_3\text{O}_4)_x$  composite thin-film optical transmittance spectra in the wavelength range of 300–1100 nm. For all deposited thin films, it was found that the transmittance increase as the wavelength increased, while transmittance decreased with increasing the concentration of the  $\text{Co}_3\text{O}_4$ , which led to a decrease in the energy gap

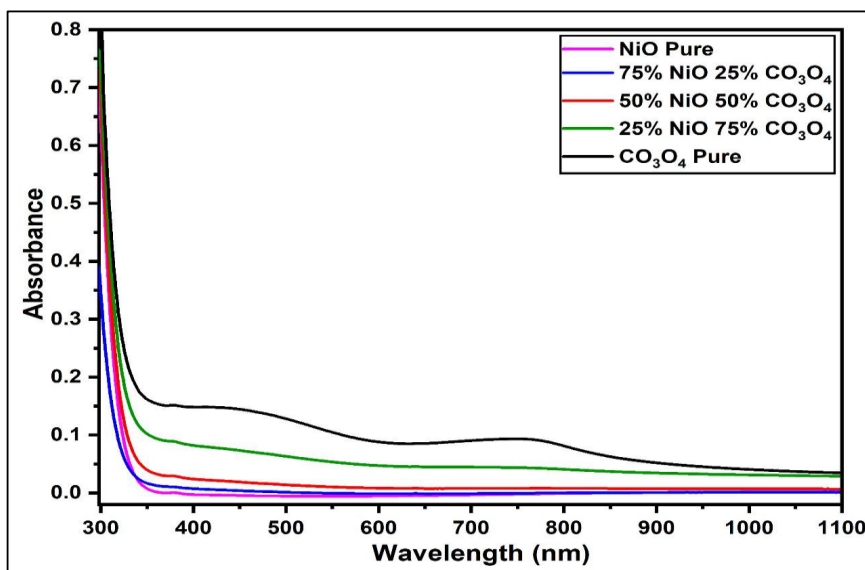


Fig. 3. absorbance spectrum for composite thin films of  $(\text{NiO})_{1-x}(\text{Co}_3\text{O}_4)_x$  at varying volumes of  $(x)$ .

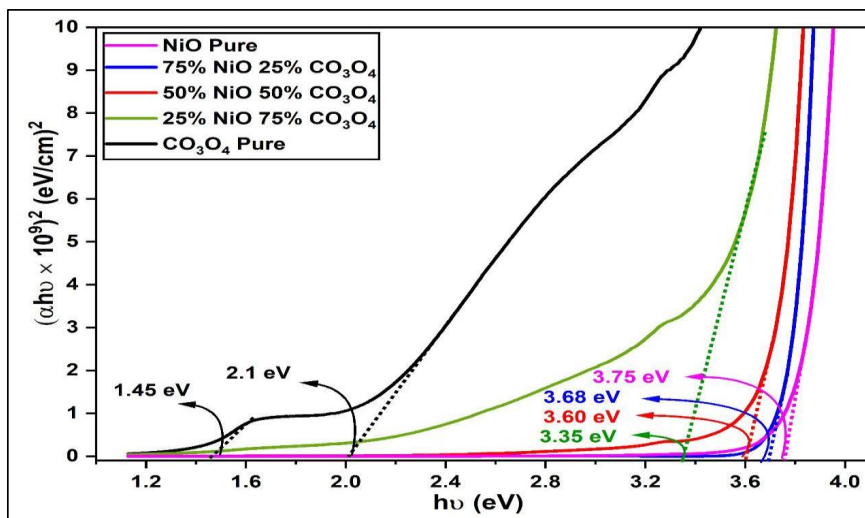


Fig. 4. Images of the energy gap for  $(\text{NiO})_{1-x}(\text{Co}_3\text{O}_4)_x$  composite thin films at varying volumes of  $(x)$ .

The values for the prepared films as in Fig. 2 are a result of the rise in the produced films' thickness as the proportion of  $\text{Co}_3\text{O}_4$  rises, which is in line with the findings of the study. [14].

Fig. 3 shows a strong absorption that subsequently dropped as the wavelength increased. In contrast, transmittance and reflectance exhibit the reverse tendency. It is evident that the films exhibited a greater capacity to absorb electromagnetic radiation at longer

wavelengths than NiO as the concentration of  $\text{Co}_3\text{O}_4$  increased. This suggests that  $\text{Co}_3\text{O}_4$  can decrease the band gap of NiO. According to the findings, the  $E_g$  value of the unaltered NiO was between (3.6 - 4) eV [15, 16].

As the concentration of  $\text{Co}_3\text{O}_4$  increased from 25% to 100%, the energy band gap of  $(\text{NiO})_{1-x}(\text{Co}_3\text{O}_4)_x$  thin films reduced from 3.75 to 2.1 eV, as illustrated in Fig. 4, where some of the unpaired electrons join with the unpaired electrons on

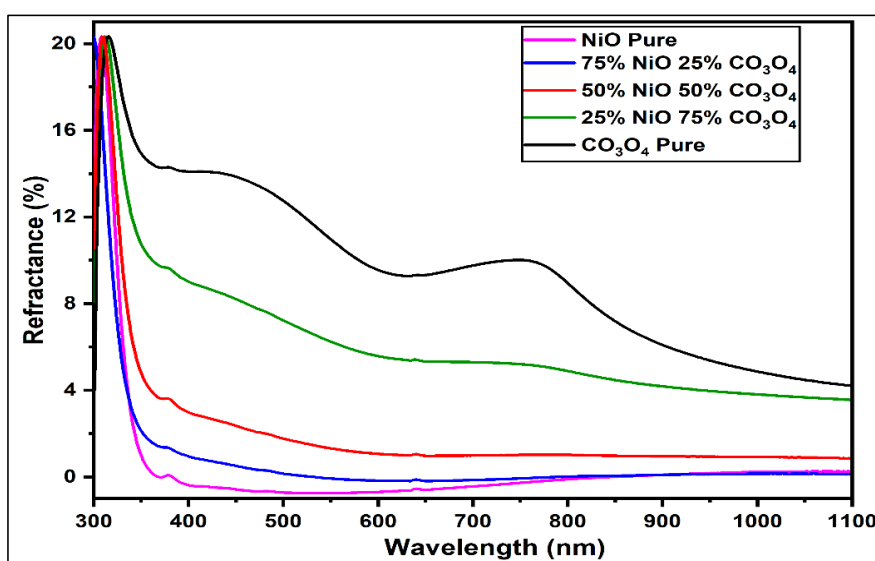


Fig. 5. Reflectance spectrum for composite thin films of  $(\text{NiO})_{1-x}(\text{Co}_3\text{O}_4)_x$  at varying volumes of (x).

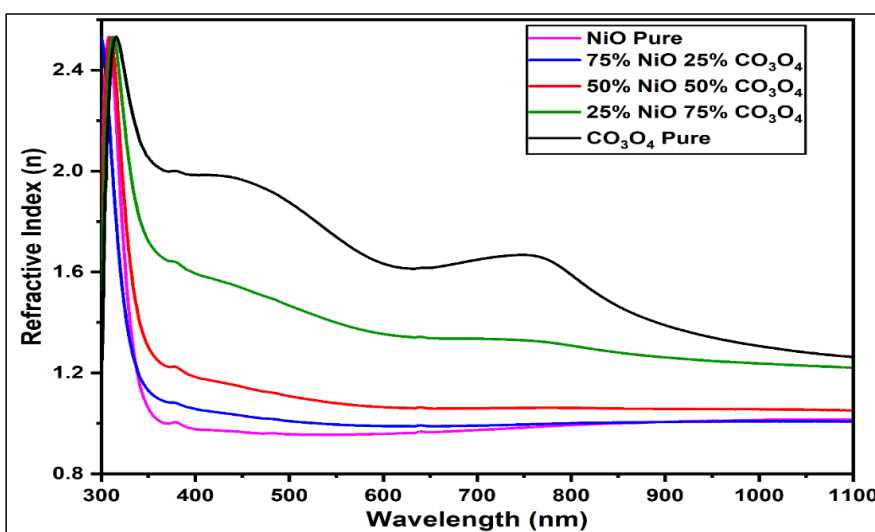


Fig. 6. Spectrum of the refractive index (n) for  $(\text{NiO})_{1-x}(\text{Co}_3\text{O}_4)_x$  composite thin films at varying volumes of (x).

the NiO surface to form a structure. The upward displacement of the valence band edge is what causes this decrease in the band gap [17–19].

We notice from the figure that with increasing the concentration of  $\text{Co}_3\text{O}_4$ , the energy gap decreases. The rise in electronic transitions can be attributed to the doping process, which produced new levels near the valence band inside the energy gap. As a result, bridges were created that made it possible for electrons to flow between the

conduction and valence bands. Consequently, the produced film's structural qualities were enhanced by the addition of  $\text{Co}_3\text{O}_4$ . The electron was unable to vaporize and travel from the valence pack to the conduction beam because the energy of the falling photon was less than the semiconductor's energy value. Consequently, raising the wavelength lowers the absorption. We note that the absorption increased with the concentration of the  $\text{Co}_3\text{O}_4$ , which led to a decrease in the energy gap values

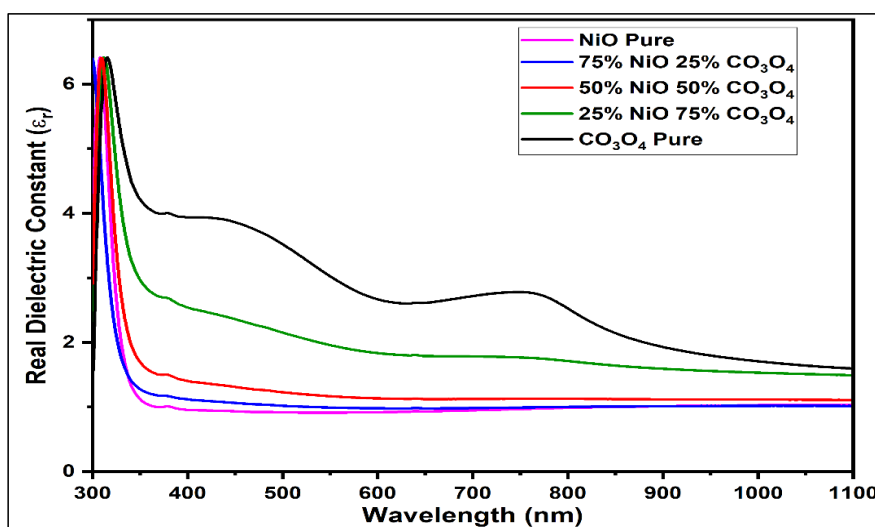


Fig. 7. The dielectric constant spectrum's real component for  $(\text{NiO})_{1-x}(\text{Co}_3\text{O}_4)_x$  composite thin films at varying volume percentages of (x).

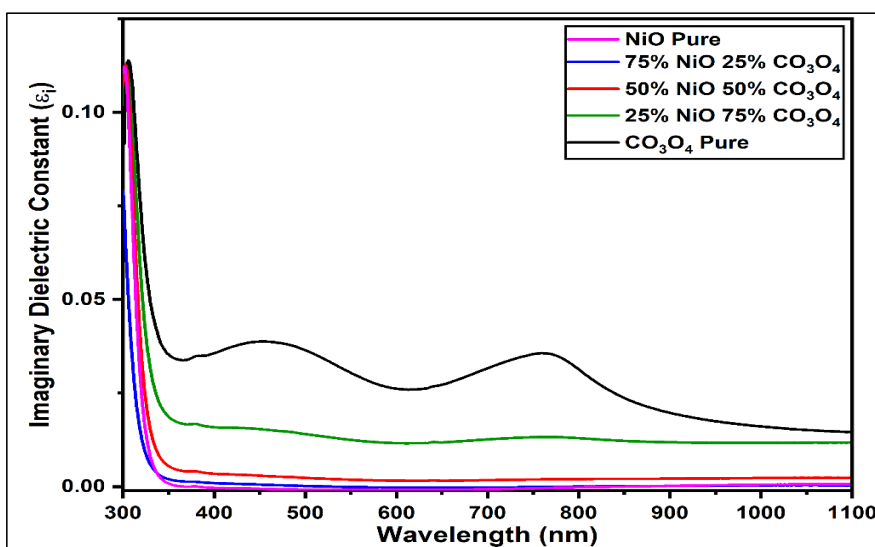


Fig. 8. The dielectric constant spectrum's imaginary component for  $(\text{NiO})_{1-x}(\text{Co}_3\text{O}_4)_x$  composite thin films at various vol.% of (x).

of the prepared films [20,21].

Fig. 5 displays the reflectance of  $(\text{NiO})_{1-x}(\text{Co}_3\text{O}_4)_x$  composite thin films. According to this figure, the reflectance rises as the  $\text{Co}_3\text{O}_4$  concentration does, which is in line with the researchers' findings [22].

It is known that the refractive index is related to reflectivity, the  $n$  results of prepared films in Fig. 6 at cutoff wavelength ( $\lambda_c$ ). It was also observed that the refractive index increases for  $\text{Co}_3\text{O}_4$  ratios this is consistent with the results of the researchers [22], which may be due to the increasing homogeneity and the surface roughness of the films.

According to [23], the dielectric constant's real ( $\epsilon_1$ ) and imaginary ( $\epsilon_2$ ) components are written as follows:

$$\epsilon_1 = n^2 - k^2 \quad (1)$$

$$\epsilon_2 = 2nk \quad (2)$$

where ( $k$ ): is the extinction coefficient and

( $n$ ): is the refractive index. The imaginary part quantifies the rate of wave dissipation in the medium, whereas the real ( $\epsilon_1$ ) component is associated with dispersion. Figs. 7 and 8 show the real and imaginary dielectric constants. Based on these figures, the values of  $\epsilon_1$  and  $\epsilon_2$  increase with increasing wavelength.

#### Dispersion Parameters

A single-term Sellmeier relation was created by Wemple and Didomenico [24] utilizing an outstanding long-wavelength approximation:

$$n^2 - 1 = E_o E_d / E_o^2 - E^2 \quad (3)$$

where ( $E_o$ ): is the single oscillator energy of the electronic transitions, ( $E_d$ ): is the dispersion energy, and  $n$  is the refractive index.

A plot of  $(n^2 - 1)^{-1}$  against  $E^2$ , see Fig. 9, was used to estimate  $E_o$  and  $E_d$  which were calculated from the slope  $(E_o E_d)^{-1}$  and intercept  $(E_o/E_d)$ . The

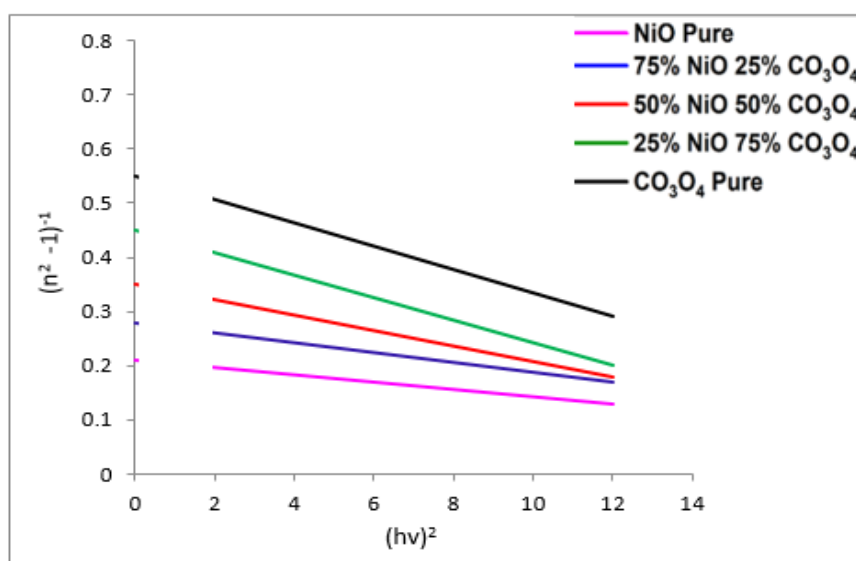


Fig. 9. For  $(\text{NiO})_{1-x}(\text{Co}_3\text{O}_4)_x$  composite thin films, plot  $(n^2 - 1)^{-1}$  against  $E^2$  as a function of photon energy squared at varying vol.% of ( $x$ ).

Table 1. the optical characteristics of composite thin films of  $(\text{NiO})_{1-x}(\text{Co}_3\text{O}_4)_x$  at varying volumes of ( $x$ ).

Samples	$E_d$ (eV)	$E_o$ (eV)	$E_g$ (eV)	$\xi$	$n_o$	$M_{-1}$	$M_{-3}(\text{eV})^{-2}$
NiO Pure	26.726	5.612	3.75	5.76	2.4	4.761	0.151
NiO <sub>75</sub> Co <sub>3</sub> O <sub>4</sub> <sub>25</sub>	19.738	5.526	3.68	4.57	2.1	3.571	0.116
NiO <sub>50</sub> Co <sub>3</sub> O <sub>4</sub> <sub>50</sub>	14.201	4.970	3.60	3.85	1.9	2.857	0.115
NiO <sub>25</sub> Co <sub>3</sub> O <sub>4</sub> <sub>75</sub>	10.327	4.647	3.35	3.22	1.7	2.222	0.102
Co <sub>3</sub> O <sub>4</sub> Pure	9.160	5.038	2.1	2.82	1.6	1.818	0.071

calculated values, which were displayed in Table (1), decreased as the concentration of  $\text{Co}_3\text{O}_4$  increased. The optical energy gap value derived from the Tauc relation was in agreement with the Wemple-DiDomenico energy gap estimate [25]. ( $n_0$ ) The static refractive index and the static dielectric constant can be obtained from the following relationships[26]:

$$n^2(o) = 1 + \frac{E_d}{E_o} \quad (4)$$

$$\epsilon = n^2(o) \quad (5)$$

The calculated values were listed in the Table (1) showing a decrease in their values with increasing concentration of the  $\text{Co}_3\text{O}_4$ .

The relationships listed below [27, 28] The ( $M_{-1}$ ) and ( $M_{-3}$ ) moments of the imaginary part of the optical spectrum of  $(\text{NiO})_{1-x}(\text{Co}_3\text{O}_4)_x$  composite thin films may be found using it:

$$E_o^2 = M_{-1}/M_{-3} \quad (6)$$

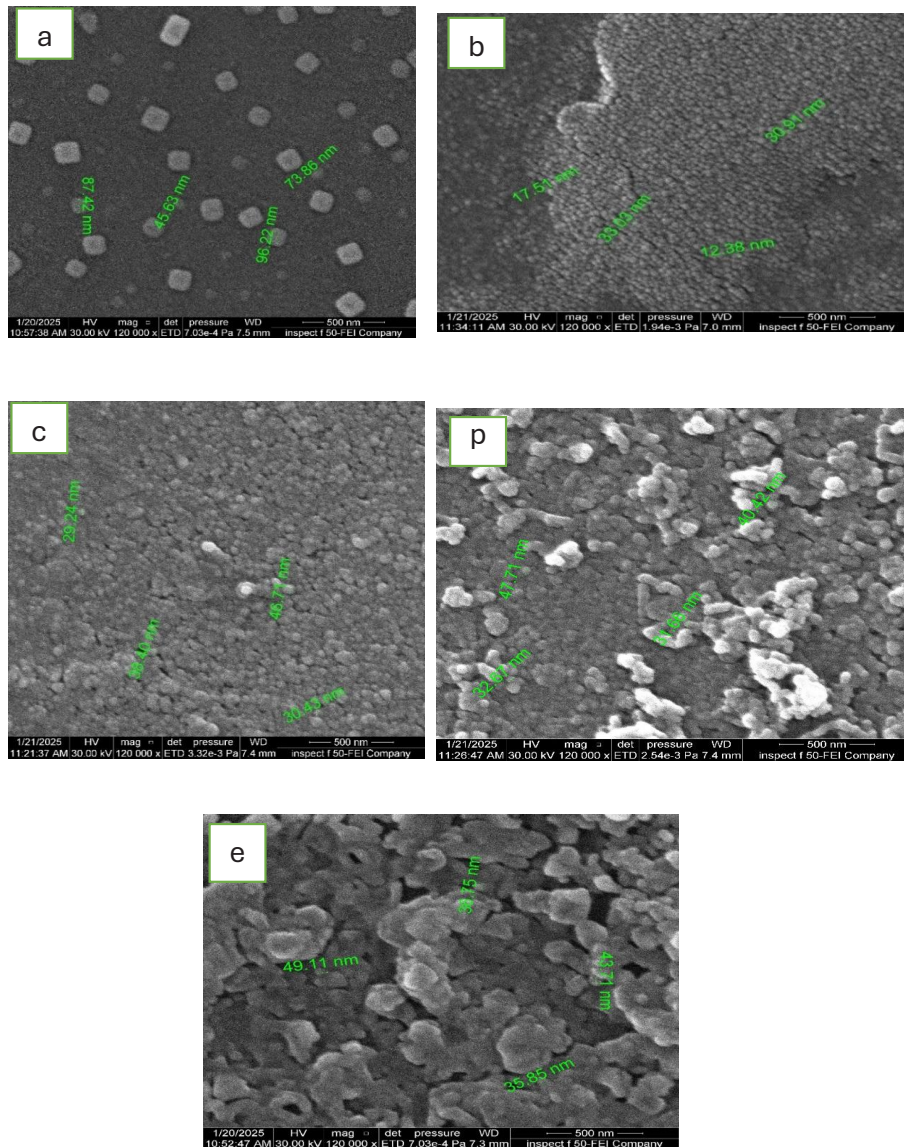


Fig. 10: FESEM pictures of composite thin films of  $(\text{NiO})_{1-x}(\text{Co}_3\text{O}_4)_x$  at varying volumes of ( $x$ ).

$$E_d^2 = M_{-1}^3 / M_{-3} \quad (7)$$

Table 1 indicates that the optical spectrum moments decrease when the concentration of  $\text{Co}_3\text{O}_4$  thin films increases.

### Structural Properties

#### Field Emission Scanning Electron Microscopy (FESEM)

FESEM images of  $(\text{NiO})_{1-x}(\text{Co}_3\text{O}_4)_x$  thin films at various  $\text{Co}_3\text{O}_4$  volume ratios (0,25,50,75, and 100)%

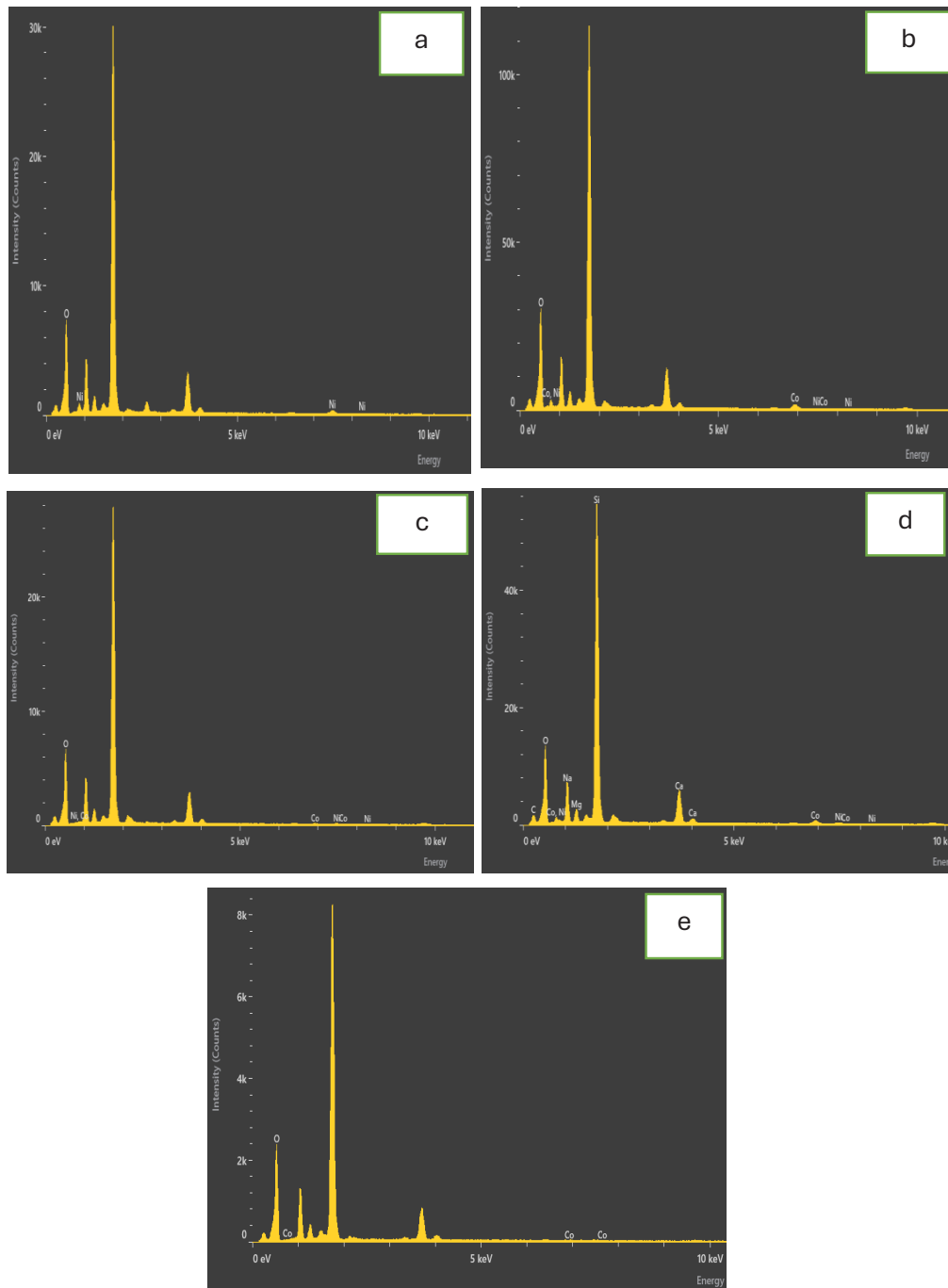


Fig. 11. EDX pictures of  $(\text{NiO})_{1-x}(\text{Co}_3\text{O}_4)_x$  composite thin films at varying vol.% of (x).

Table 2. EDX analysis for prepared films elements compositions.

Samples	Element	Weight %	Atomic %
NiO Pure	O	90.3	97.2
	Ni	9.7	2.8
NiO <sub>75</sub> Co <sub>3</sub> O <sub>4</sub> <sub>25</sub>	O	87.4	96.2
	Co	11.1	3.3
	Ni	1.6	0.5
	O	94.5	98.4
NiO <sub>50</sub> Co <sub>3</sub> O <sub>4</sub> <sub>50</sub>	Co	2.1	0.6
	Ni	3.4	1.0
	O	86.5	95.9
	Co	9.4	2.8
NiO <sub>25</sub> Co <sub>3</sub> O <sub>4</sub> <sub>75</sub>	Ni	4.2	1.3
	O	99.0	99.7
	Co	1.0	0.3
Co <sub>3</sub> O <sub>4</sub> Pure	O	99.0	99.7
	Co	1.0	0.3

are displayed in Fig. 10.(a-e). As can be seen, thin films share a common surface form with several  $\text{Co}_3\text{O}_4$  aggregates or chunks arranged haphazardly on the top surface. The image displays a cubic nanocrystal. The results indicate that  $\text{Co}_3\text{O}_4$  had a propensity to cluster and disperse effectively in the  $(\text{NiO})_{1-x}(\text{Co}_3\text{O}_4)_x$  thin films. Cobalt oxide developed a continuous network with  $(\text{NiO})_{1-x}(\text{Co}_3\text{O}_4)_x$  as its concentration rose. The findings presented herein are consistent with the conclusions reached [29]. From the Fig. 10, we notice that the size of the particles in the membranes is nano-sized, which means that the membranes can be used as a sensing application because the nano-sized size provides a high adsorption area, and this is one of the conditions for high sensitivity, this is consistent with the work of researchers. [30]

#### Energy Dispersive X-ray Spectroscopy (EDX)

Fig. 11 (a-e) shows the energy-dispersive X-ray analysis (EDX) spectra of the  $(\text{NiO})_{1-x}(\text{Co}_3\text{O}_4)_x$  thin films that were formed on a glass substrate. Fig. 4 shows the  $(\text{NiO})_{1-x}(\text{Co}_3\text{O}_4)_x$  thin films' energy-dispersive X-ray analysis (EDX) spectrum for various  $\text{Co}_3\text{O}_4$  concentrations (0,25,50,75, and 100)% that were deposited on a glass substrate using the spray pyrolysis approach. The components Ni, O, and Co

were found to be highly prevalent. Additionally, as seen in Table 2.

#### CONCLUSION

Using 0.05 M of  $\text{NiCl}_2 \cdot 6\text{H}_2\text{O}$  and 0.05 M of  $\text{CoCl}_2 \cdot 6\text{H}_2\text{O}$  diluted in distilled water, the chemical spray pyrolysis approach has successfully produced the  $(\text{NiO})_{1-x}(\text{Co}_3\text{O}_4)_x$  composite thin films. As the concentration of  $\text{Co}_3\text{O}_4$  grows, the reflectance, real and imaginary dielectric constants, and refractive index all rise. This could be because the films become more homogeneous and rough on the surface, which makes them appropriate for sensing applications. As the concentration of  $\text{Co}_3\text{O}_4$  in the  $(\text{NiO})_{1-x}(\text{Co}_3\text{O}_4)_x$  composite thin films increases, dispersion parameters decrease also. Energy dispersive X-ray spectroscopy (EDX), the analysis revealed the prominent presence of the components Ni, O, and Co, field emission scanning electron microscopy (FESEM), It can be noted thin films have a common surface shape comprising many randomly placed chunks or aggregates of  $\text{Co}_3\text{O}_4$  on the top surface of the films.

#### CONFLICT OF INTEREST

The authors declare that there is no conflict of interests regarding the publication of this

manuscript.

## REFERENCES

1. Aghazadeh M. Synthesis, characterization, and study of the supercapacitive performance of NiO nanoplates prepared by the cathodic electrochemical deposition-heat treatment (CED-HT) method. *Journal of Materials Science: Materials in Electronics*. 2016;28(3):3108-3117.
2. Agrawal S, Parveen A, Azam A. Microwave assisted synthesis of Co doped NiO nanoparticles and its fluorescence properties. *J Lumin*. 2017;184:250-255.
3. Chougule MA, Pawar SG, Godse PR, Mulik RN, Sen S, Patil VB. Synthesis and Characterization of Polypyrrole (PPy) Thin Films. *Soft Nanoscience Letters*. 2011;01(01):6-10.
4. Shelke PN, Kholam YB, Hawaldar RR, Gunjal SD, Udawant RR, Sarode MT, et al. Synthesis, characterization and optical properties of selective  $\text{Co}_3\text{O}_4$  films 1-D interlinked nanowires prepared by spray pyrolysis technique. *Fuel*. 2013;112:542-549.
5. Chen J, Wu X, Selloni A. Electronic structure and bonding properties of cobalt oxide in the spinel structure. *Physical Review B*. 2011;83(24).
6. Zhou T, Zhang T, Deng J, Zhang R, Lou Z, Wang L. P-type  $\text{Co}_3\text{O}_4$  nanomaterials-based gas sensor: Preparation and acetone sensing performance. *Sensors Actuators B: Chem*. 2017;242:369-377.
7. Mohamed WM. Effect of Lasing Energy on Optical and Structural Properties of (ZnS) Nanostructured Thin Films for Solar Cell Applications. *Neuroquantology*. 2020;18(5):29-34.
8. Khalaf AJ. Investigation and Prepared of  $\text{Cu}_2\text{ZnSnS}_4$  Compound Films as a Gas Sensor by Pulse Laser Deposition. *Neuroquantology*. 2020;18(1):117-123.
9. Xia XH, Tu JP, Zhang J, Xiang JY, Wang XL, Zhao XB. Fast electrochromic properties of self-supported  $\text{Co}_3\text{O}_4$  nanowire array film. *Sol Energy Mater Sol Cells*. 2010;94(2):386-389.
10. Rajeshkhanna G, Umeshbabu E, Rao GR. In situ grown nano-architectures of  $\text{Co}_3\text{O}_4$  on Ni-foam for charge storage application. *Journal of Chemical Sciences*. 2016;129(2):157-166.
11. AlSultani MJ, Alias MFA. Influence of GO concentration on photoconversion efficiency for dye-sensitized solar cells using  $\text{GO}:\text{TiO}_2$ -AD as photoanodes. *Experimental and Theoretical NANOTECHNOLOGY*. 2025;9(5):103-114.
12. Khan ZR, Alshammari AS, Shkir M. Role of Zn doping in improving opto-nonlinear and photodetection properties of spray pyrolysis grown  $\text{Cd}_{1-x}\text{Zn}_x\text{S}$  nanostructured thin films. *Radiat Phys Chem*. 2024;216:111382.
13. Idan MH, Kadhim RG, Mohammed MA. Retraction: Preparation and study of the effect of adding cobalt and magnesium on the morphological, optical properties and bacterial activity of cadmium sulfide compound. *AIP Conference Proceedings: AIP Publishing*; 2023. p. 040117.
14. Farhan MM, Khodair ZT, Ibrahim BA. Study of the Structural and Optical Properties of Ni-doped  $\text{Co}_3\text{O}_4$  Thin Films Using Chemical Spray Pyrolysis Technique. *IOP Conference Series: Materials Science and Engineering*. 2020;871(1):012090.
15. Louardi A, Rmili A, Ouachtari F, Bouaoud A, Elidrissi B, Erguig H. Characterization of cobalt oxide thin films prepared by a facile spray pyrolysis technique using perfume atomizer. *J Alloys Compd*. 2011;509(37):9183-9189.
16. Patil SL, Chougule MA, Pawar SG, Sen S, Patil VB. Effect of Camphor Sulfonic Acid Doping on Structural, Morphological, Optical and Electrical Transport Properties on Polyaniline-ZnO Nanocomposites. *Soft Nanoscience Letters*. 2012;02(03):46-53.
17. Manogowri R, Mary Mathelane R, Valanarasu S, Kulandaisamy I, Benazir Fathima A, Kathalingam A. Effect of annealing temperature on the structural, morphological, optical and electrical properties of  $\text{Co}_3\text{O}_4$  thin film by nebulizer spray pyrolysis technique. *Journal of Materials Science: Materials in Electronics*. 2015;27(4):3860-3866.
18. Abbas SZ, Aboud AA, Irfan M, Alam S. Effect of substrate temperature on structure and optical properties of  $\text{Co}_3\text{O}_4$  films prepared by spray pyrolysis technique. *IOP Conference Series: Materials Science and Engineering*. 2014;60:012058.
19. Hassan AJ. Study of Optical and Electrical Properties of Nickel Oxide (NiO) Thin Films Deposited by Using a Spray Pyrolysis Technique. *Journal of Modern Physics*. 2014;05(18):2184-2191.
20. Hasan NB, Jasim Mohammed M. Structural and Morphological Studies of  $(\text{NiO})/(\text{CuO})$  Thin Films Prepared by Chemical Spray Pyrolysis Technique. *International Letters of Chemistry, Physics and Astronomy*. 2015;58:102-112.
21. Seshendra Reddy C, Sivasankar Reddy A, Sreedhara Reddy P. Influence of substrate temperature on the electrical, morphological and structural properties of electron beam evaporated LBMO thin films. *Electronic Materials Letters*. 2014;10(1):159-163.
22. A Electrical and Optical Characteristics of Stannous Doped Nickel Oxide Thin Film Formed by Spray Pyrolysis Technique. *International Journal of Innovative Technology and Exploring Engineering*. 2019;8(12S2):406-409.
23. Lu H-C, Chu C-L, Lai C-Y, Wang Y-H. Property variations of direct-current reactive magnetron sputtered copper oxide thin films deposited at different oxygen partial pressures. *Thin Solid Films*. 2009;517(15):4408-4412.
24. Wemple SH. Refractive-Index Behavior of Amorphous Semiconductors and Glasses. *Physical Review B*. 1973;7(8):3767-3777.
25. Alfayhan AS, Hasan NB. Influence of Pulse Laser Deposition on the Structural and Optical Properties of CZTS for Sensor Applications. *Revue des composites et des matériaux avancés*. 2024;34(1):95-102.
26. Mohammed HRA, Al-Ogaili AOM, Abass KH. Structural and dispersion parameters of nano-layers prepared from Al-Ni-Cr alloy. *Materials Today: Proceedings*. 2023;80:3296-3304.
27. Fe Doped  $\text{WO}_3$  Thin films Prepared by Spray Pyrolysis towards Ethanol Sensing. *International Journal of ChemTech Research*. 2018.
28. Bendová P, Karmanská A. Comparison Of Kindergarten and Primary School Teachers' Approach To Children At Risk Of Developing Sld in the Czech Republic and Abroad. *EDULEARN Proceedings*; 2018/07: IATED; 2018. p. 9994-10000.
29. Soltani S, Rozati SM, Askari MB. Optical and electrochemical properties of spinel cubic nanostructured thin film  $\text{Co}_3\text{O}_4$  prepared by spray pyrolysis. *Physica B: Condensed Matter*. 2022;625:413464.
30. Ashok Kumar Reddy Y, Ajitha B, Sreedhara Reddy P, Siva Pratap Reddy M, Lee J-H. Effect of substrate temperature on structural, optical and electrical properties of sputtered NiO-Ag nanocrystalline thin films. *Electronic Materials Letters*. 2014;10(5):907-913.